Spectral properties of Titan's impact craters imply chemical weathering of its surface

Catherine D. Neish, Jason W. Barnes, C. Sotin, S. Mackenzie, J. M. Soderblom, Stéphane Le Mouélic, R.L. Kirk, B.W. Stiles, M.J. Malaska, Alice Le Gall, et al.

AGU PUBLICATIONS

Geophysical Research Letters

RESEARCH LETTER
10.1002/2015GL063824

Key Points:
- We examine the spectral properties of Titan's impact craters
- Degraded crater rims are more enriched in water ice than fresh crater rims
- Observations suggest chemical weathering of organics in water ice matrix

Correspondence to:
C. D. Neish,
cneish@fit.edu

Citation:
Neish, C. D., et al. (2015), Spectral properties of Titan's impact craters imply chemical weathering of its surface, *Geophys. Res. Lett.*, *42*, 3746–3754, doi:10.1002/2015GL063824.

Received 12 MAR 2015
Accepted 23 APR 2015
Accepted article online 20 MAY 2015
Published online 26 MAY 2015

Spectral properties of Titan's impact craters imply chemical weathering of its surface

C. D. Neish[1], J. W. Barnes[2], C. Sotin[3], S. MacKenzie[2], J. M. Soderblom[4], S. Le Mouélic[5], R. L. Kirk[6], B. W. Stiles[3], M. J. Malaska[3], A. Le Gall[7], R. H. Brown[8], K. H. Baines[3], B. Buratti[3], R. N. Clark[9], and P. D. Nicholson[10]

[1]Department of Physics and Space Sciences, Florida Institute of Technology, Melbourne, Florida, USA, [2]Department of Physics, University of Idaho, Moscow, Idaho, USA, [3]Jet Propulsion Laboratory, California Institute of Technology, Pasadena, California, USA, [4]Department of Earth, Atmospheric and Planetary Sciences, Massachusetts Institute of Technology, Cambridge, Massachusetts, USA, [5]Laboratoire de Planétologie et Géodynamique, LPGNantes, CNRS UMR 6112, Université de Nantes, Nantes, France, [6]United States Geological Survey, Astrogeology Science Center, Flagstaff, Arizona, USA, [7]Laboratoire Atmosphères, Milieux, Observations Spatiales (LATMOS), Université de Versailles Saint-Quentin, Paris, France, [8]Lunar and Planetary Laboratory, University of Arizona, Tucson, Arizona, USA, [9]United States Geological Survey, Denver, Colorado, USA, [10]Department of Astronomy, Cornell University, Ithaca, New York, USA

Abstract We examined the spectral properties of a selection of Titan's impact craters that represent a range of degradation states. The most degraded craters have rims and ejecta blankets with spectral characteristics that suggest that they are more enriched in water ice than the rims and ejecta blankets of the freshest craters on Titan. The progression is consistent with the chemical weathering of Titan's surface. We propose an evolutionary sequence such that Titan's craters expose an intimate mixture of water ice and organic materials, and chemical weathering by methane rainfall removes the soluble organic materials, leaving the insoluble organics and water ice behind. These observations support the idea that fluvial processes are active in Titan's equatorial regions.

1. Introduction

The Visual and Infrared Mapping Spectrometer (VIMS) [*Brown et al.*, 2004] on the Cassini spacecraft has observed the surface of Titan in seven atmospheric windows in the near infrared [*Sotin et al.*, 2005]. These observations have shown that the surface of Titan is spectrally diverse [*Rodriguez et al.*, 2006; *Barnes et al.*, 2007a; *McCord et al.*, 2008]. For example, one spectral unit on Titan is highly correlated with organic sand particles forming large dune fields, as observed by Cassini RADAR [*Soderblom et al.*, 2007; *Rodriguez et al.*, 2014]. Another spectral unit is found primarily on the edges of lakes and the bottom of dry lakebeds and has been interpreted to be areas of evaporites [*Barnes et al.*, 2011; *MacKenzie et al.*, 2014]. Based on reflectance values at 1.28, 1.57, and 2.03 μm, some areas have been interpreted as being enriched in water ice [*Le Mouélic et al.*, 2008]. There is also a widespread spectral unit, known as the equatorial bright terrains, with an unknown composition. The spectral units tend to have a strong latitudinal dependence, with most dune units within 30° of the equator and many evaporitic units found near the poles.

The observed variations in composition are somewhat surprising, given that Titan's atmosphere supports active photochemistry. These reactions produce an organic haze that settles to the surface [e.g., *Lavvas et al.*, 2008], and a few-micron-thick layer of such aerosols could obscure the visible and infrared spectrum of any underlying material. The spectral variety indicates that Titan has a surface actively modified by exogenic and possibly endogenic processes [e.g., *Jaumann et al.*, 2009; *Lopes et al.*, 2013; *Aharonson et al.*, 2014]. To determine the composition of Titan's upper crustal layer, one must therefore look at features that have been exposed in the recent past. Impact craters are capable of probing the subsurface, so the rims, ejecta blankets, and central uplifts of the freshest craters should represent the composition of Titan's upper crust (similar inferences have been made on other planetary bodies, such as the Moon [e.g., *McEwen et al.*, 1994]). A crater's excavation depth is roughly one tenth the transient diameter [*Melosh*, 1989], so for the craters considered here (which all have final diameters >40 km, or correspondingly, transient diameters >30 km [*Neish and Lorenz*, 2012]), this translates to excavation depths of several kilometers.

Models of Titan's internal structure suggest that its crust is water ice rich [e.g., *Tobie et al*., 2005], but detecting spectral evidence for water ice on the surface of Titan through its atmosphere is difficult. Patterns of absorption within the VIMS spectral windows have been used to claim that the "dark blue" spectral unit represents local enhancements in water ice abundance [*Rodriguez et al*., 2006; *Barnes et al*., 2007a; *Soderblom et al*., 2007]. However, *Clark et al*. [2010] noted that the strong 3 μm water ice absorption feature will result in a negative spectral slope from 2.7 to 2.8 μm for any water ice exposed on Titan and that every VIMS spectrum acquired of Titan shows a positive slope between these wavelengths. New measurements of atmospheric transmission show that Titan's atmosphere absorbs more strongly at 2.7 μm than it does at 2.8 μm [*Barnes et al*., 2013; *Hayne et al*., 2014], so the raw I/F measured by VIMS may not represent the true surface reflectivity at 2.7 μm. A full radiative transfer analysis is needed to confirm the quantitative effect of the atmospheric absorption on surface reflectivities. For the purposes of this paper we interpret the dark blue spectral signature to represent areas enhanced in water ice.

Intriguingly, the material exposed in the rims of fresh impact craters does not appear to be the most water ice-rich material found on Titan. Sinlap is one of the freshest craters on Titan, with a depth comparable to similarly sized craters on Ganymede, implying minimal degradation by erosional processes [*Neish et al*., 2013a]. However, its rim, ejecta blanket, and central uplift are not composed of the dark blue spectral unit thought to represent water ice-rich material [*Le Mouélic et al*., 2008]. Rather, they are characterized by a "bright green" spectral unit of unknown composition, similar to the equatorial bright terrains. *Soderblom et al*. [2007] proposed that this spectral unit represents a deposit of bright, fine, precipitating aerosols but that fails to explain why Sinlap—a feature known to be relatively young—looks spectrally similar to the equatorial bright terrains that are presumably much older. It also fails to explain why Sinlap shows any spectral diversity at all and is not uniformly coated in aerosols.

In this work, we analyze the spectral properties of a sample of Titan's impact craters to infer their evolution over time and observe how craters change as exogenic processes modify them. The results help to constrain the composition of Titan's upper crust, as well as the primary processes working to degrade its surface.

2. Observations

VIMS uses spectral image mapping to obtain images in 352 colors [*Brown et al*., 2004]. VIMS' wavelength range, 0.3–5.2 μm, includes windows centered at 0.94, 1.08, 1.28, 1.6, 2.0, 2.7, 2.8, and 5.0 μm, where neither haze nor atmospheric absorption completely obscures Titan's surface. The windows have varying spectral widths; the 2.7 and 2.8 μm windows are essentially one channel wide (~0.02 μm), whereas the 2.0 and 5.0 μm windows are roughly six and 16 channels wide, respectively. Combinations of these windows enable the production of false color images of the surface of Titan. In this work, we use a color scheme (red: average over 4.8–5.2 μm, green: 2.00 μm, and blue: 1.28 μm) that has been previously used to distinguish between Titan's main geologic units [e.g., *Barnes et al*., 2007a], such as sand dunes, evaporites, and equatorial bright terrain (Figure 1a).

We examined three craters in a range of degradation states (Table 1). All three craters have been observed by both Cassini RADAR and VIMS and have depth estimates from either synthetic aperture radar topography (SARTopo) profiles or stereo topography [*Stiles et al*., 2009; *Neish et al*., 2013a, 2013b]. We use the relative depth of the crater, $R(D)$, as a proxy for degradation state. Relative depth is defined as $R(D) = 1 - d_t(D)/d_g(D)$, where $d_t(D)$ is the depth of a crater with diameter D on Titan and $d_g(D)$ is the depth of a crater with diameter D on Ganymede [*Schenk*, 2002; *Bray et al*., 2012]. A relative depth of zero indicates the crater is as deep as a similarly sized crater on Ganymede, while a relative depth of one indicates that the crater is completely flat [*Neish et al*., 2013a]. Craters with small relative depths are therefore less degraded than craters with large relative depths. Even if fresh craters on Titan are systematically shallower than fresh craters on Ganymede (i.e., due to a different crustal rheology), the relative depth reported here still provides a reasonable proxy for the relative degradation state of craters on Titan.

The least degraded crater we examined is Sinlap (11.3°N, 16.1°W), with a relative depth of 0.4 ± 0.2 (Figures 1b–1d). It is characterized by a spectrally dark blue interior and a spectrally bright green rim and ejecta blanket, with a spectrally dark blue unit found to the east of the crater. *Le Mouélic et al*. [2008] interpret this latter unit as an area possibly enriched in water ice, which formed as the result of redeposition of an icy vapor plume blown downwind. However, they cannot account for the spectral

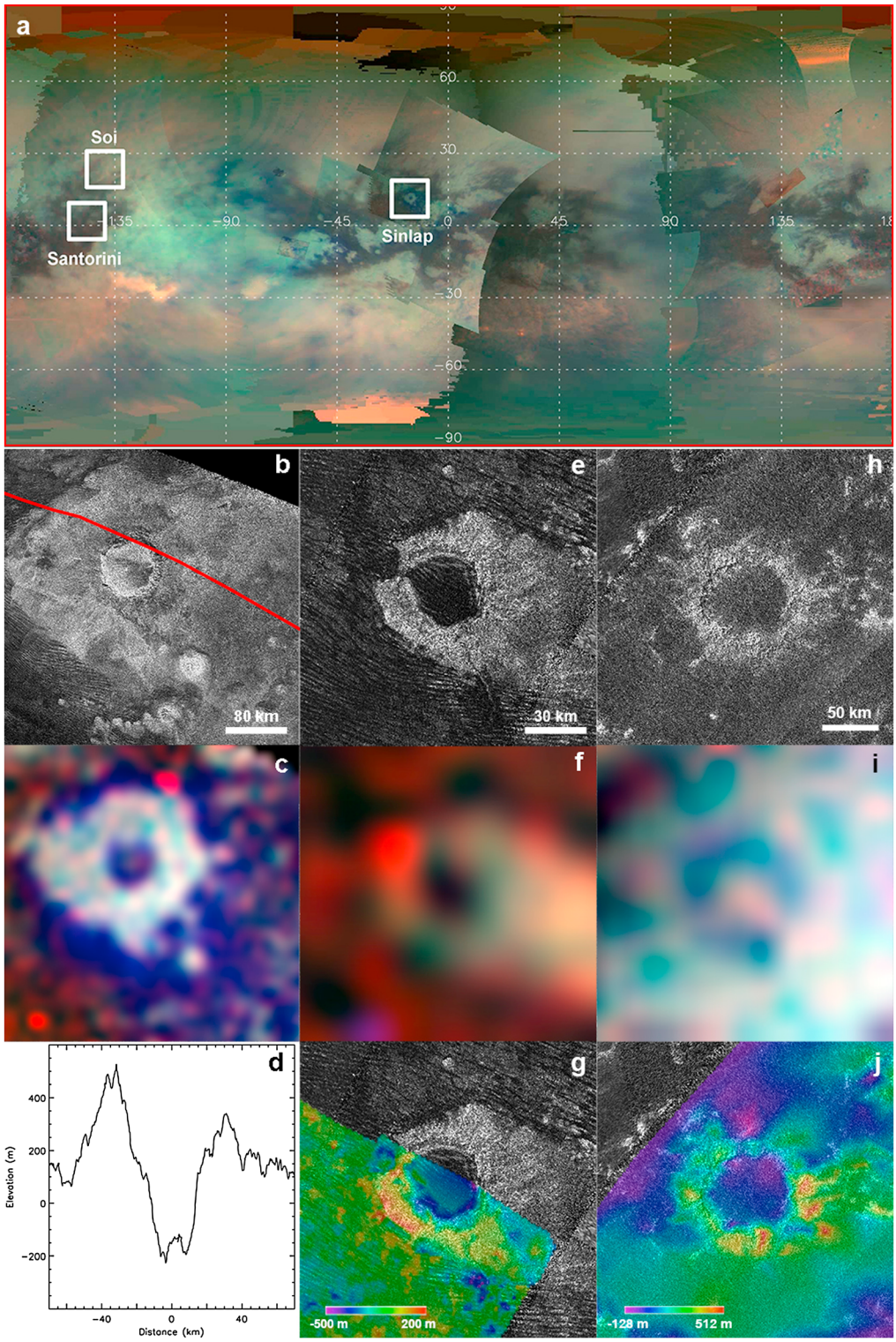

Figure 1. (a) Mosaic of Cassini VIMS observations of Titan in simple cylindrical projection. Colors are mapped with 4.8–5.2 μm as red, 2.00 μm as green, and 1.28 μm as blue. The locations of the three craters studied in this work are marked with white boxes. The 5 μm bright regions observed at high latitudes are clouds. (b) RADAR and (c) VIMS images of Sinlap crater, the least degraded crater in this study. (d) Synthetic aperture radar topography (SARTopo) profile through the northern edge of Sinlap crater, as reported in *Neish et al.* [2013a]. Profile line shown in red in Figure 1b. (e) RADAR and (f) VIMS images of the crater in Santorini Facula with (g) partial digital terrain model. Dunes are seen on the crater floor in Figure 1e. (h) RADAR and (i) VIMS images of Soi crater, the flattest known crater on Titan. (j) A digital terrain model of Soi indicates a depth of only 240 ± 120 m.

Table 1. Depth Measurements for the Craters Studied in This Work[a]

Crater	Diameter D (km)	Depth d (m)[b]	Relative Depth R[c]	Relative Depth R[d]	Spectral Unit		
					Rim and Ejecta	Floor	Central Uplift
Sinlap	82 ± 2	640^{+160}_{-150}	$0.43^{+0.14}_{-0.13}$	$0.36^{+0.16}_{-0.15}$	Bright green, with small patches of dark blue	Dark blue, with small unit of dark brown	Bright green
Santorini	40 ± 5	340 ± 70	0.61 ± 0.08	0.70 ± 0.06	Bright green	Dark brown	NA
Soi	78 ± 2	240 ± 120	0.78 ± 0.10	0.76 ± 0.11	Dark blue	Bright green	NA

[a]NA, not applicable.
[b]The depth measurement for Sinlap is from *Neish et al*. [2013a]. The depth measurement for Soi is from *Neish et al*. [2013b]. This is the first reported measurement of the depth of Santorini.
[c]Ganymede crater depths from Table 4 in *Bray et al*. [2012].
[d]Ganymede crater depths from Figure 2b in *Schenk* [2002].

appearance of the ejecta blanket: "Sinlap's nearby ejecta blanket […] shows no spectral digressions from any of the rest of the equatorial bright material. This, in itself, is remarkable: a feature known to be relatively young that nevertheless looks the same as much older terrains." The rim of Sinlap is presumably some of the freshest material exposed on the surface of Titan, yet it appears less enriched in water ice than many other areas on Titan, including its own crater floor. *Le Mouélic et al*. [2008] also observe the remnants of a central uplift on Sinlap's floor, with a spectral signature similar to its ejecta blanket. They infer this to mean that the impact target site was vertically homogeneous over its excavation depth.

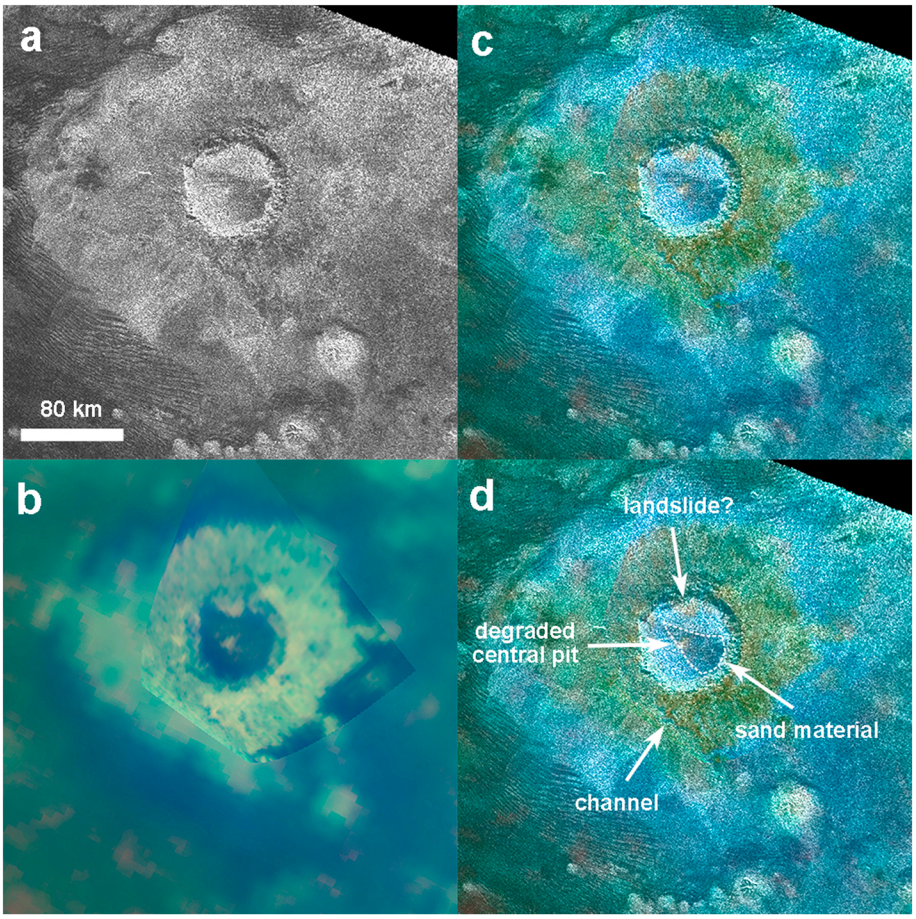

Figure 2. (a) Cassini RADAR image of Sinlap crater. (b) New Cassini VIMS image of Sinlap crater, acquired with a pixel scale that ranges between ~1 and 4 km (CM_1790056808_1), placed over a lower resolution image of the same region (CM_1525118253_1). The color scheme is the same as that in Figure 1. (c) RADAR image colorized with VIMS data. (d) Annotated version of the colorized RADAR image. Features discussed in the text are indicated with white arrows.

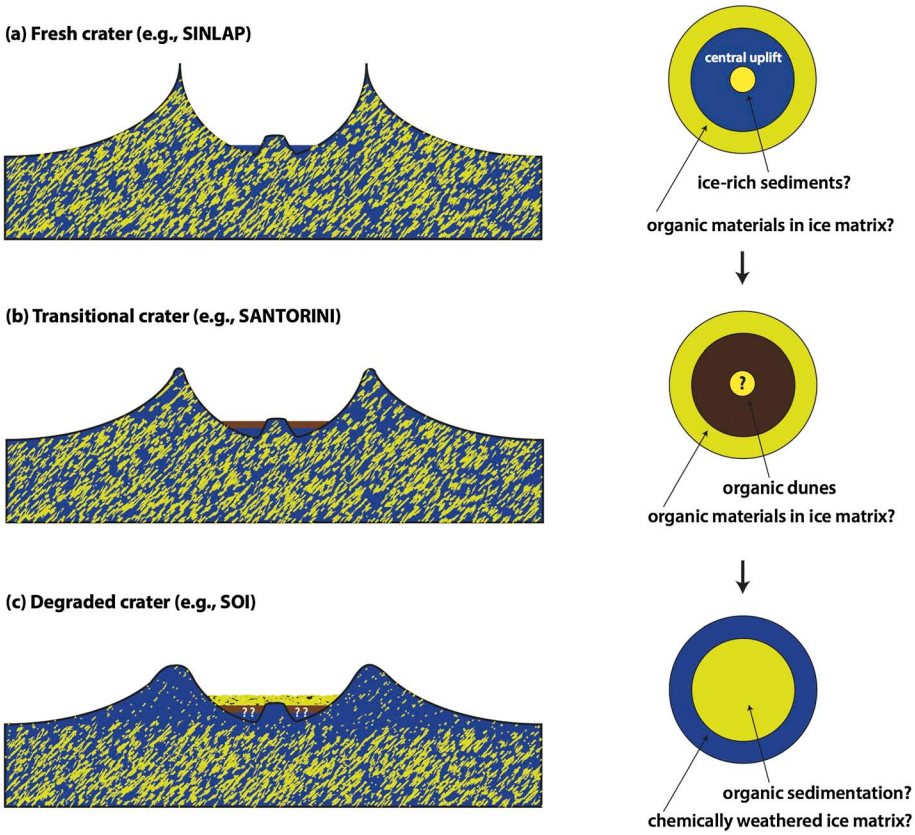

Figure 3. (a–c) A proposed progression of impact crater degradation on Titan, as seen in (left) side view and (right) plan view. Blue materials are inferred to be water ice rich, brown materials are correlated with regions of sand dunes, and yellowish-green materials represent an as-yet unknown material, presumably more enriched in organic material.

A new fine-resolution VIMS image of Sinlap was acquired during the T105 flyby on 22 September 2014 (Figure 2). This cube has one of the longest integration times (160 ms) for a VIMS cube acquired from low altitude. Due to the observational geometry and long integration time, the resolution of the data varies significantly across the image, becoming finer as Cassini approached Titan. The sampling is better than 1 km/pixel southwest of the crater floor in Figure 2b. (For comparison, the sampling was limited to 13 km/pixel in the data presented in *Le Mouélic et al.* [2008].) The result is one of the highest signal-to-noise VIMS views of Titan's surface that exists at fine resolution, making it ideal for both geomorphic and spectroscopic investigations. In targeting and tracking Sinlap over the course of the observation, the spacecraft slewed to keep the crater within the field of view. Therefore, the emission angle varies significantly across the image, from 47° at the start (northeast of crater in Figure 2b) to 20° at the end (southwest of crater in Figure 3b). The solar incidence angle at Sinlap during the time of the observation was 22°.

This image reveals additional morphological constraints not evident in the coarser-resolution VIMS data or the RADAR data (Figure 2). The overall morphology of Sinlap strongly suggests that it has been subject to some amount of fluvial erosion. It has a flat floor, the presence of a degraded and mostly absent central uplift, and evidence of a large channel in the ejecta blanket. A portion of the northern rim also appears to have slumped onto the crater floor in a possible landslide. This area is radar bright, consistent with centimeter-scale debris, and spectrally bright green, similar to the surrounding rim and ejecta blanket. The remainder of the radar-bright portions of the crater floor is spectrally dark blue, consistent with a water ice-rich sediment. The spectrally bright green ejecta blanket itself is heterogeneous in spectral character, with small spectrally dark blue units imbedded within it. A topographic profile through the rim and ejecta blanket suggests that it is more than 100 m higher than the surrounding terrain (Figure 1d), so the spectral variations may be consistent with variations in the extent of erosion of the ejecta blanket. Finally, there is

new evidence for infilling by a thin layer of sand on the crater floor. The radar-dark portion of the crater floor is spectrally similar to the spectrally "dark brown" sand material.

Craters that are more degraded than Sinlap, such as the crater in Santorini Facula (2.2°N, 147.7°W) ($R = 0.65 \pm 0.12$), are characterized by a spectrally dark brown interior and a spectrally bright green rim (Figures 1e–1g). In the case of the crater Paxsi, *Buratti et al.* [2012] attributed a spectrally dark brown interior to infilling by dune material. This interpretation is strongly supported in the case of Santorini, where dune forms are observed in the crater interior in the high-resolution RADAR image (Figure 1e). As in the case of Sinlap, the rim and ejecta blanket are spectrally similar to the nearby equatorial bright terrain.

Finally, Soi, the shallowest known crater on Titan (24.3°N, 141.0°W) ($R = 0.8 \pm 0.1$) is characterized by a spectrally bright green interior and a spectrally dark blue rim (Figures 1h–1j). Soi is roughly the same size as Sinlap but has no evidence of a central uplift. We interpret Soi to be an extremely degraded crater, which may have been subject to both fluvial erosion and aeolian infilling. The observed depth of Soi, 0.24 ± 0.11 km, supports the idea that it was partially (if not completely) modified by fluvial erosion [*Neish et al.*, 2013b]. Aeolian infilling tends to leave the crater rim largely clear of deposits, while fluvial erosion lowers the rim through mechanical erosion [*Forsberg-Taylor et al.*, 2004]. The unmodified rim of Soi should be between 0.3 and 1.2 km in height [*Bray et al.*, 2012], so its observed height of 0.24 ± 0.11 km suggests that some mechanical erosion took place. There is also no spectral signature of the dark brown equatorial dune material in the crater interior. Soi is located beyond the northern margin of Titan's Shangri-La sand sea, so it is possible that Soi was never filled in by dark brown sand. If it was filled in by sand, spectrally bright green sediments have since coated this spectrally dark brown material.

3. Discussion

The VIMS observations suggest an evolutionary sequence for Titan's impact craters that includes both mechanical erosion and chemical weathering (Figure 3). We propose that the rims, ejecta blankets, and central uplifts of fresh impact craters on Titan are composed of an insoluble matrix whose cracks and pores are filled with a soluble organic material, producing a bright green spectral response. The craters undergo rapid erosion by fluvial processes and mass wasting, removing evidence of central uplifts and filling the crater floor with sediments [*Neish et al.*, 2013b]. During this process, mechanical weathering reduces the crater's depth while methane rainfall dissolves the organic materials, leaving the dark blue insoluble matrix intact. The crater interior may then be filled with dark brown wind-deposited materials, and eventually, bright green organic sediments washed off the crater walls. Water ice is one material that is consistent with the spectrally dark blue insoluble matrix, since it is highly resistant to chemical weathering by organic solvents [*Lorenz and Lunine*, 1996]. The composition of the soluble organic material is unknown, but theoretical estimates of the equilibrium solubilities of many of Titan's organic materials suggest that they may be as soluble in methane as common cave forming materials on Earth are in water [*Malaska and Hodyss*, 2014].

The origin of the fractured water ice matrix is unclear. Since the central uplifts and rims of Titan's craters are sourced from the top few kilometers of its crust, one interpretation is that it is representative of Titan's upper crustal composition. This suggestion is supported by atmospherically corrected images of Titan's surface. These show large regions on Titan that are spectrally consistent with a mixture of water ice and hydrocarbons [*Hayne et al.*, 2014]. The suggestion that Titan's upper crust is composed of fractured water ice, and organics is distinct from the inference that Titan's upper crust is composed of methane or ethane clathrate [*Tobie et al.*, 2006; *Choukroun and Sotin*, 2012]. The spectrum of methane clathrate is nearly identical to water ice in this wavelength range [*Smythe*, 1975], so the two compounds would be indistinguishable in the color scheme used in this work. Further evidence for large amounts of organic material on Titan's surface comes from radiometry [*Janssen et al.*, 2009], which is consistent with the presence of high emissivity substances such as organic compounds covering much of Titan's surface. Limited regions of low emissivity substances, consistent with fractured water ice, are also observed.

It is unclear what process could mix organics and ice to the depths sampled by Titan's impact craters. If the porosity of Titan's surface is 0.5 at the surface, it would drop to near 0.2 at 4 km depth [*Kossacki and Lorenz*, 1996]. The porosity would be even smaller at the depth sampled by Sinlap ($1/10\, D_t \sim 5$ km) due to compaction, which may limit the ability of organics to percolate down to these regions. For comparison,

the Moon has a surface porosity of 20% that decreases with depth, reaching zero porosity by 15–25 km [*Besserer et al*., 2014]. If Titan had a photochemically active atmosphere early in its history when the rate of impact cratering was likely higher [*Artemieva and Lunine*, 2005], it is possible that the atmospherically produced organics could have been intimately mixed with water ice in a deep megaregolith. *Tobie et al*. [2006] predict that Titan had such a methane-rich atmosphere > 3 Ga.

An alternative hypothesis is that the fractured water ice formed during the impact itself and the spectral signature of Titan's impact craters changed through the chemical alteration of the host rock in a hydrothermal system. Hydrothermal activity appears to be common on terrestrial planets after impact into water-rich surfaces [*Naumov*, 2002], and the same may be true for Titan, where there is extensive evidence for liquid hydrocarbons on its surface [e.g., *Niemann et al*., 2005; *Stofan et al*., 2007]. In terrestrial impact craters where hydrothermal alteration has occurred (such as Haughton crater in northern Canada), hydrothermal deposits are most common in the interiors of central uplifts, the edge of the impact melt sheet, the heavily fractured outer margin of the central uplift, and the faulted rim region [*Osinski et al*., 2005]. Hydrothermal alteration is also thought to have occurred in Toro crater on Mars, and the hydrothermal deposits there are predominantly associated with the central uplift and portions of the crater floor [*Marzo et al*., 2010]. On Titan, organic materials could circulate with liquid water, forming exotic organic molecules, including those containing oxygen [*Neish et al*., 2010], and deposit material in the crater's fractures and faults, changing the spectral signature of its rim and central uplift. The widths of Titan's crater rims are considerably larger than similar craters on Ganymede, which may further suggest induration of crater ejecta by hydrocarbons. Insoluble organic materials may precipitate out of any liquid mixed with the ejecta, producing a coating resistant to erosion, similar to the mechanism thought to produce pedestal craters on Mars [*Barlow et al*., 2000].

The evolutionary sequence proposed here provides a reasonable source for the sediments needed for the mechanical erosion of Titan's surface [*Collins*, 2005; *Burr et al*., 2006]. Methane rainfall could dissolve some of the soluble organic materials, leaving the more insoluble organic materials and water ice behind as an abrasive material. The proposed evolutionary sequence also allows us to make predictions about the relative depths of craters based on their spectra alone. For example, Selk crater has a similar spectral signature to Sinlap [*Soderblom et al*., 2010], so we predict that the SARTopo profiles generated for this crater will show it to have a relative depth similar to Sinlap. Preliminary measurements suggest a depth of 470 ± 90 m ($R = 0.56 \pm 0.13$) for Selk, which is shallower than Sinlap, but within errors. Forseti (formerly Crater #5 from *Wood et al*. [2010]), looks spectrally similar to Soi crater. We further predict that the stereo topography of this crater will reveal it to have a large relative depth. Preliminary measurements suggest a depth of 180 ± 60 m ($R = 0.85 \pm 0.15$), consistent with these predictions.

An alternative explanation for the VIMS observations reported here is that no chemical weathering has occurred and the composition of the crater rims and central uplifts are simply representative of the target material. Sinlap and Santorini are both located in Titan's equatorial sand seas, while Soi is located near the edge of Titan's undifferentiated plains (Figure 1a) [*Lopes et al*., 2010]. An intimate mixture of organic sand materials and water ice may lead to the spectrally bright green appearance in Sinlap's ejecta blanket, while Soi may be exposing an unaltered water ice substrate. On a global scale, there are areas in Titan's equatorial regions that also appear spectrally dark blue [*Le Mouélic et al*., 2012; *Rodriguez et al*., 2014], including several regions associated with mountains [*Barnes et al*., 2007b]. This may lend support to the chemical weathering hypothesis, since elevated regions are more likely to be "washed clean" by methane rainfall. Similarly, the equatorial bright terrains may remain spectrally bright green because they are located in topographic lows and serve as sediment sinks for Titan's organic materials. However, not all mountains are dark blue and not all dark blue units are mountains, so it is unclear whether the spectral response of the mountains is representative of the underlying crust or their degradation state. A global study of the spectral response of Titan's mountains is needed to distinguish between the two hypotheses.

Another test of the chemical weathering hypothesis would be the identification of a degraded, spectrally dark blue crater in the sand seas and/or a fresh, spectrally bright green crater in the plains. This would imply that the crustal composition of Titan is relatively uniform, and it is simply weathering that causes the observed changes in the craters' spectral properties. Unfortunately, it is difficult to deconvolve the effects of increased fluvial erosion from the effects of the different substrates; most "fresh" craters are located in

the sand seas, and most "degraded" craters are located poleward of ~20° in the undifferentiated plains [*Neish et al*., 2013a], where fluvial erosion may be more common. In addition, many of Titan's craters are too small to resolve with the Cassini VIMS instrument. A high-resolution infrared imager (possibly on an airborne platform [*Barnes et al*., 2012]) would aid in distinguishing between these two hypotheses.

4. Conclusions

The spectral properties of Titan's impact craters suggest that chemical weathering has been an active process in its equatorial regions. Fresh craters are formed with rims, ejecta blankets, and central uplifts that are less enriched in water ice than the rims of the most degraded craters on Titan. This is consistent with a scenario where Titan's craters expose an intimate mixture of water ice and organic materials, and chemical weathering by methane rainfall removes the soluble organic materials, leaving the insoluble organics and water ice behind. This suggests that Titan's upper crust is a fractured water ice bedrock whose cracks and pores have been filled in by organic materials, or alternatively, that high-energy impacts induce hydrothermal alteration of the target rock shortly after crater formation. Chemical weathering of this material provides a reasonable source for the sediments required for the mechanical weathering of Titan's surface.

Acknowledgments
We wish to acknowledge the Cassini VIMS and RADAR teams for acquiring and processing the data presented here. Data from the Cassini mission are made publicly available through the Planetary Data System (pds.nasa.gov). We also wish to thank E. Turtle and an anonymous individual for their careful reviews and J. Lunine for input that helped to improve the manuscript. C.N. and C.S. acknowledge support from the NASA Outer Planets Research Program (NNH11ZDA001N-OPR and NNH13ZDA001N-OPR). Part of this work was performed at the Jet Propulsion Laboratory, California Institute of Technology under contract with NASA.

The Editor thanks Elizabeth Turtle and an anonymous reviewer for their assistance in evaluating this paper.

References

Aharonson, O., A. G. Hayes, R. Lopes, A. Lucas, P. Hayne, and J. T. Perron (2014), Titan's surface geology, in *Titan: Surface, Atmosphere and Magnetosphere*, edited by I. Mueller-Wodarg et al., pp. 43–75, Cambridge Univ. Press, Cambridge, U. K.

Artemieva, N., and J. I. Lunine (2005), Impact cratering on Titan II. Global melt, escaping ejecta, and aqueous alteration of surface organics, *Icarus*, *175*, 522–533, doi:10.1016/j.icarus.2004.12.005.

Barlow, N. G., J. M. Boyce, F. M. Costard, R. A. Craddock, J. B. Garvin, S. E. Sakimoto, R. O. Kuzmin, D. J. Roddy, and L. A. Soderblom (2000), Standardizing the nomenclature of Martian impact crater ejecta morphologies, *J. Geophys. Res.*, *105*, 26,733–26,738, doi:10.1029/2000JE001258.

Barnes, J. W., R. H. Brown, L. Soderblom, B. J. Buratti, C. Sotin, S. Rodriguez, S. Le Mouélic, K. H. Baines, R. Clark, and P. Nicholson (2007a), Global-scale surface spectral variations on Titan seen from Cassini/VIMS, *Icarus*, *186*, 242–258, doi:10.1016/j.icarus.2006.08.021.

Barnes, J. W., et al. (2007b), Near-infrared spectral mapping of Titan's mountains and channels, *J. Geophys. Res.*, *112*, E11006, doi:10.1029/2007JE002932.

Barnes, J. W., et al. (2011), Organic sedimentary deposits in Titan's dry lakebeds: Probable evaporate, *Icarus*, *216*, 136–140, doi:10.1016/j.icarus.2011.08.022.

Barnes, J. W., et al. (2012), AVIATR—Aerial Vehicle for In-situ and Airborne Titan Reconnaissance: A Titan airplane mission concept, *Exp. Astron.*, *33*, 55–127, doi:10.1007/s10686-011-9275-9.

Barnes, J. W., et al. (2013), A transmission spectrum of Titan's North Polar Atmosphere from a specular reflection of the Sun, *Astrophys. J.*, *777*, 161, doi:10.1088/0004-637X/777/2/161.

Besserer, J., F. Nimmo, M. A. Wieczorek, R. C. Weber, W. S. Kiefer, P. J. McGovern, J. C. Andrews-Hanna, D. E. Smith, and M. T. Zuber (2014), GRAIL gravity constraints on the vertical and lateral density structure of the lunar crust, *Geophys. Res. Lett.*, *41*, 5771–5777, doi:10.1002/2014GL060240.

Bray, V. J., P. M. Schenk, H. J. Melosh, J. V. Morgan, and G. S. Collins (2012), Ganymede crater dimensions—Implications for central peak and central pit formation and development, *Icarus*, *217*(1), 115–129, doi:10.1016/j.icarus.2011.10.004.

Brown, R. H., et al. (2004), The Cassini Visual and Infrared Mapping Spectrometer (VIMS) investigation, *Space Sci. Rev.*, *115*, 111–168, doi:10.1007/s11214-004-1453-x.

Buratti, B. J., C. Sotin, K. Lawrence, R. H. Brown, S. Le Mouélic, J. M. Soderblom, J. Barnes, R. N. Clark, K. H. Baines, and P. D. Nicholson (2012), A newly discovered impact crater in Titan's Senkyo: Cassini VIMS observations and comparison with other impact features, *Planet. Space Sci.*, *60*, 18–25, doi:10.1016/j.pss.2011.05.004.

Burr, D., J. Emery, R. Lorenz, G. Collins, and P. Carling (2006), Sediment transport by liquid surficial flow: Application to Titan, *Icarus*, *181*(1), 235–242, doi:10.1016/j.icarus.2005.11.012.

Choukroun, M., and C. Sotin (2012), Is Titan's shape caused by its meteorology and carbon cycle?, *Geophys. Res. Lett.*, *39*, L04201, doi:10.1029/2011GL050747.

Clark, R. N., et al. (2010), Detection and mapping of hydrocarbon deposits on Titan, *J. Geophys. Res.*, *115*, E10005, doi:10.1029/2009JE003369.

Collins, G. C. (2005), Relative rates of fluvial bedrock incision on Titan and Earth, *Geophys. Res. Lett.*, *32*, L22202, doi:10.1029/2005GL024551.

Forsberg-Taylor, N. K., A. D. Howard, and R. A. Craddock (2004), Crater degradation in the Martian highlands: Morphometric analysis of the Sinus Sabaeus region and simulation modeling suggest fluvial processes, *J. Geophys. Res.*, *109*, E05002, doi:10.1029/2004JE002242.

Hayne, P. O., T. B. McCord, and C. Sotin (2014), Titan's surface composition and atmospheric transmission with solar occultation measurements by Cassini VIMS, *Icarus*, *243*, 158–172, doi:10.1016/j.icarus.2014.08.045.

Janssen, M. A., et al. (2009), Titan's surface at 2.2-cm wavelength imaged by the Cassini RADAR radiometer: Calibration and first results, *Icarus*, *200*, 222–239, doi:10.1016/j.icarus.2008.10.017.

Jaumann, R., et al. (2009), Geology and surface processes on Titan, in *Titan From Cassini-Huygens*, edited by R. H. Brown, J.-P. Lebreton, and J. H. Waite, pp. 75–140, Springer, New York.

Kossacki, K. J., and R. D. Lorenz (1996), Hiding Titan's ocean: Densification and hydrocarbon storage in an icy regolith, *Planet. Space Sci.*, *44*, 1029–1037, doi:10.1016/0032-0633(96)00022-0.

Lavvas, P. P., A. Coustenis, and I. M. Vardavas (2008), Coupling photochemistry with haze formation in Titan's atmosphere. Part II: Results and validation with Cassini/Huygens data, *Planet. Space Sci.*, *56*, 67–99, doi:10.1016/j.pss.2007.05.027.

Le Mouélic, S., et al. (2008), Mapping and interpretation of Sinlap crater on Titan using Cassini VIMS and RADAR data, *J. Geophys. Res.*, *113*, E04003, doi:10.1029/2007JE002965.

Le Mouélic, S., et al. (2012), Global mapping of Titan's surface using an empirical processing method for the atmospheric and photometric correction of Cassini/VIMS images, *Planet. Space Sci.*, *73*, 178–190, doi:10.1016/j.pss.2012.09.008.

Lopes, R. M. C., et al. (2010), Distribution and interplay of geologic processes on Titan from Cassini radar data, *Icarus*, *205*, 540–558, doi:10.1016/j.icarus.2009.08.010.
Lopes, R. M. C., et al. (2013), Cryovolcanism on Titan: New results from Cassini RADAR and VIMS, *J. Geophys. Res.-Planets*, *118*, 416–435, doi:10.1002/jgre.20062.
Lorenz, R. D., and J. I. Lunine (1996), Erosion on Titan: Past and present, *Icarus*, *122*, 79–91, doi:10.1006/icar.1996.0110.
MacKenzie, S. M., et al. (2014), Evidence of Titan's climate history from evaporite distribution, *Icarus*, *243*, 191–207, doi:10.1016/j.icarus.2014.08.022.
Malaska, M. J., and R. Hodyss (2014), Dissolution of benzene, naphthalene, and biphenyl in a simulated Titan lake, *Icarus*, *242*, 74–81, doi:10.1016/j.icarus.2014.07.022.
Marzo, G. A., A. F. Davila, L. L. Tornabene, J. M. Dohm, A. G. Fairén, C. Gross, T. Kneissl, J. L. Bishop, T. L. Roush, and C. P. McKay (2010), Evidence for Hesperian impact-induced hydrothermalism on Mars, *Icarus*, *208*, 667–683, doi:10.1016/j.icarus.2010.03.013.
McCord, T. B., et al. (2008), Titan's surface: Search for spectral diversity and composition using the Cassini VIMS investigation, *Icarus*, *194*(1), 212–242, doi:10.1016/j.icarus.2007.08.039.
McEwen, A. S., M. S. Robinson, E. M. Eliason, P. G. Lucey, T. C. Duxbury, and P. D. Spudis (1994), Clementine observations of the Aristarchus region of the Moon, *Science*, *266*, 1858–1862, doi:10.1126/science.266.5192.1858.
Melosh, H. J. (1989), *Impact Cratering*, Oxford Univ. Press, Oxford, U. K.
Naumov, M. V. (2002), Impact-generated hydrothermal systems: Data from Popigai, in *Kara and Puchezh-Katunki Impact Structure in Impacts in Precambrian Shield*, edited by J. Plado and L. J. Pesonen, pp. 117–171, Springer, Berlin, Germany.
Neish, C. D., and R. D. Lorenz (2012), Titan's global crater population: A new assessment, *Planet. Space Sci.*, *60*, 26–33, doi:10.1016/j.pss.2011.02.016.
Neish, C. D., Á. Somogyi, and M. A. Smith (2010), Titan's primordial soup: Formation of amino acids via low-temperature hydrolysis of tholins, *Astrobiology*, *10*, 337–347, doi:10.1089/ast.2009.0402.
Neish, C. D., R. L. Kirk, R. D. Lorenz, V. J. Bray, P. Schenk, B. W. Stiles, E. Turtle, K. Mitchell, A. Hayes, and Cassini RADAR team (2013a), Crater topography on Titan: Implications for landscape evolution, *Icarus*, *223*, 82–90, doi:10.1016/j.icarus.2012.11.030.
Neish, C. D., et al. (2013b), *The Unusual Crater Soi on Titan: Possible Formation Scenarios, Paper Presented at the 44th Lunar and Planetary Science Conference*, Lunar and Planetary Institute, The Woodlands, Tex.
Niemann, H. B., et al. (2005), The abundances of constituents of Titan's atmosphere from the GCMS instrument on the Huygens probe, *Nature*, *438*, 779–784, doi:10.1038/nature04122.
Osinski, G. R., P. Lee, J. Parnell, J. G. Spray, and M. Baron (2005), A case study of impact-induced hydrothermal activity: The Haughton impact structure Devon Island, Canadian High Arctic, *Meteorit. Planet. Sci.*, *40*, 1859–1877, doi:10.1111/j.1945-5100.2005.tb00150.x.
Rodriguez, S., et al. (2006), Cassini/VIMS hyperspectral observations of the Huygens landing site on Titan, *Planet. Space Sci.*, *54*, 1510–1523, doi:10.1016/j.pss.2006.06.016.
Rodriguez, S., et al. (2014), Global mapping and characterization of Titan's dune fields with Cassini: Correlation between RADAR and VIMS observations, *Icarus*, *230*, 168–179, doi:10.1016/j.icarus.2013.11.017.
Schenk, P. (2002), Thickness constraints on the icy shells of the Galilean satellites from a comparison of crater shapes, *Nature*, *417*, 419–421, doi:10.1038/417419a.
Smythe, W. D. (1975), Spectra of hydrate frosts: Their application to the outer solar system, *Icarus*, *24*, 421–427, doi:10.1016/0019-1035(75)90059-7.
Soderblom, J. M., et al. (2010), Geology of the Selk crater region on Titan from Cassini VIMS observations, *Icarus*, *208*, 905–912, doi:10.1016/j.icarus.2010.03.001.
Soderblom, L. A., et al. (2007), Correlations between Cassini VIMS spectra and RADAR SAR images: Implications for Titan's surface composition and the character of the Huygens Probe Landing Site, *Planet. Space Sci.*, *55*, 2025–2036, doi:10.1016/j.pss.2007.04.014.
Sotin, C., et al. (2005), Release of volatiles from a possible cryovolcano from near-infrared imaging of Titan, *Nature*, *435*, 786–789, doi:10.1038/nature03596.
Stiles, B. W., et al. (2009), Determining Titan surface topography from Cassini SAR data, *Icarus*, *202*, 584–598, doi:10.1016/j.icarus.2009.03.032.
Stofan, E. R., et al. (2007), The lakes of Titan, *Nature*, *445*, 61–64, doi:10.1038/nature05438.
Tobie, G., O. Grasset, J. I. Lunine, A. Mocquet, and C. Sotin (2005), Titan's internal structure inferred from a coupled thermal-orbital model, *Icarus*, *175*, 496–502, doi:10.1016/j.icarus.2004.12.007.
Tobie, G., J. I. Lunine, and C. Sotin (2006), Episodic outgassing as the origin of atmospheric methane on Titan, *Nature*, *440*, 61–64, doi:10.1038/nature04497.
Wood, C. A., R. Lorenz, R. Kirk, R. Lopes, K. Mitchell, E. Stofan, and the Cassini RADAR Team (2010), Impact craters on Titan, *Icarus*, *206*, 334–344, doi:10.1016/j.icarus.2009.08.021.